

MoDitector: Module-Directed Testing for Autonomous Driving Systems

RENZHI WANG^{*†}, University of Alberta, Canada
 MINGFEI CHENG^{*}, Singapore Management University, Singapore
 XIAOFEI XIE, Singapore Management University, Singapore
 YUAN ZHOU[‡], Zhejiang Sci-Tech University, China
 LEI MA, The University of Tokyo & University of Alberta, Japan

Testing Autonomous Driving Systems (ADS) is crucial for ensuring their safety, reliability, and performance. Despite numerous testing methods available that can generate diverse and challenging scenarios to uncover potential vulnerabilities, these methods often treat ADS as a black-box, primarily focusing on identifying system failures like collisions or near-misses without pinpointing the specific modules responsible for these failures. Understanding the root causes of failures is essential for effective debugging and subsequent system repair. We observed that existing methods also fall short in generating diverse failures that adequately test the distinct modules of an ADS, such as perception, prediction, planning and control.

To bridge this gap, we introduce *MoDitector*, the first root-cause-aware testing method for ADS. Unlike previous approaches, *MoDitector* not only generates scenarios leading to collisions but also showing which specific module triggered the failure. This method targets specific modules, creating test scenarios that highlight the weaknesses of these given modules. Specifically, our approach involves designing module-specific oracles to ascertain module failures and employs a module-directed testing strategy that includes module-specific feedback, adaptive seed selection, and mutation. This strategy guides the generation of tests that effectively provoke module-specific failures. We evaluated *MoDitector* across four critical ADS modules and four testing scenarios. The results demonstrate that our method can effectively and efficiently generate scenarios where errors in targeted modules are responsible for ADS failures. It generates 216.7 expected scenarios in total, while the best-performing baseline detects only 79.0 scenarios. Our approach represents a significant innovation in ADS testing by focusing on identifying and rectifying module-specific errors within the system, moving beyond conventional black-box failure detection.

Additional Key Words and Phrases: Module-Specific Failure, Autonomous Driving System, Testing

ACM Reference Format:

Renzhi Wang, Mingfei Cheng, Xiaofei Xie, Yuan Zhou, and Lei Ma. 2025. *MoDitector*: Module-Directed Testing for Autonomous Driving Systems. 1, 1 (February 2025), 21 pages. <https://doi.org/10.1145/nnnnnnnn.nnnnnnnn>

^{*}Both authors contributed equally to this research.

[†]This work was done during the author's visit to Singapore Management University

[‡]Corresponding author.

Authors' Contact Information: [Renzhi Wang](#), University of Alberta, Edmonton, Alberta, Canada, renzhi.wang@ualberta.ca; [Mingfei Cheng](#), Singapore Management University, Singapore, Singapore, mfcheng.2022@smu.edu.sg; [Xiaofei Xie](#), Singapore Management University, Singapore, Singapore, xfxie@smu.edu.sg; [Yuan Zhou](#), Zhejiang Sci-Tech University, Hangzhou, Zhejiang, China, zhouyuan1130@163.com; [Lei Ma](#), The University of Tokyo & University of Alberta, Tykyo, Japan, ma.lei@acm.org.

Permission to make digital or hard copies of all or part of this work for personal or classroom use is granted without fee provided that copies are not made or distributed for profit or commercial advantage and that copies bear this notice and the full citation on the first page. Copyrights for components of this work owned by others than the author(s) must be honored. Abstracting with credit is permitted. To copy otherwise, or republish, to post on servers or to redistribute to lists, requires prior specific permission and/or a fee. Request permissions from permissions@acm.org.

© 2025 Copyright held by the owner/author(s). Publication rights licensed to ACM.

ACM XXXX-XXXX/2025/2-ART

<https://doi.org/10.1145/nnnnnnnn.nnnnnnnn>

1 Introduction

Autonomous Driving Systems (ADSs) have rapidly advanced in recent years, aiming to enhance transportation and urban mobility. ADSs act as the brain of autonomous vehicles (AVs), processing extensive sensor data (e.g., images, LiDAR points) through various modules (e.g., perception, prediction, planning, and control) to operate vehicles. ADSs are considered highly safety-critical systems, as they have demonstrated vulnerability to critical issues arising from minor perturbations in the driving environment. For example, Tesla’s Autopilot system has been involved in multiple accidents where it failed to recognize stationary emergency vehicles, leading to crashes and prompting federal investigations [14]. Therefore, ADSs require extensive testing to ensure their safety and reliability during real-world deployment.

ADS testing can be broadly divided into *real-world testing* and *simulation-based testing*. Real-world testing is necessary, but it is impractical and costly due to the vast number of miles required and the rarity of critical events. In contrast, simulation-based testing offers a controllable, efficient, and cost-effective environment for both developing and testing autonomous vehicles (AVs), allowing for the creation and testing of diverse scenarios that would be difficult to reproduce in real-world conditions. In recent years, significant efforts have been made to advance simulation-based testing for ADSs to identify potential system failures such as collision and timeout. Specifically, existing studies have primarily focused on reconstructing scenarios from real-world data [15, 29, 44] or developing search algorithms [8, 37, 48] to generate safety-critical scenarios.

An ADS typically comprises multiple modules, including perception, prediction, planning, and control, each tasked with specific functions. Recent research [33] underscores the importance of understanding the root causes of detected failures, which poses challenges in effectively detecting scenarios that reflect diverse root causes. While current methods can identify numerous safety-critical scenarios, they often treat the ADS as a black box. It remains unclear *which specific module leads to a failure and how the diversity of generated failures accurately reflects the weaknesses of different modules*. Existing black-box testing methods may be biased toward detecting failures predominantly caused by weaker modules, such as those in planning or perception, thus not providing a understanding and comprehensive view of all potential weaknesses (see results in Section 3.2). Detecting failures across various modules is crucial for developers to understand the root causes accurately and enhance the corresponding components effectively.

One might question whether it is sufficient to test individual modules within an ADS, such as evaluating the object detection model in the perception module. Indeed, some studies [34, 49] have focused on model-level evaluations, testing specific modules like perception. However, model errors do not always lead to system failures, and the multiple modules within an ADS can often tolerate some model errors (refer to Section 3.2). For instance, an error in the perception module to detect a distant vehicle may not necessarily lead to a system failure, such as a collision, particularly if the missed vehicle does not impact the trajectory of the ego vehicle. Therefore, a more effective approach to ADS testing should generate diverse *system-level* failure, which can pinpoint the limitations of individual modules. It is the primary goal of this paper.

To fill this gap, we aim to investigate the generation of ADS system failures—critical scenarios predominantly triggered by specific modules, such as perception, prediction, planning and control. We define these scenarios as “Module-Induced Critical Scenarios” (MICS), which are safety-critical scenarios revealing system-level failures caused by malfunctions within a designated module \mathcal{M} . For instance, consider a collision precipitated by a mis-detection in the perception module while other modules operate correctly. Nonetheless, generating MICS for a particular module \mathcal{M} presents two primary challenges: ❶ The first challenge is the lack of effective oracles for identifying MICS. Intuitively, generating MICS requires the target module to exhibit errors while other modules

function correctly. This necessitates an oracle capable of accurately determining whether a module is malfunctioning or operating as intended. For example, the interactive nature of modules in ADSs complicates the attribution of failures, making it difficult to discern whether a failure originates from the planning module or upstream modules like perception and prediction. ❷ Another challenge lies in effectively and efficiently generating *MICSs* considering the complex interactions of multiple modules. For instance, most existing methods rely on safety-critical feedback, such as minimizing distance to collision, which may not effectively generate *MICS* for the given target module, M . As noted earlier, the optimization process in testing tools may be biased towards identifying failures induced by the least robust module, rather than the target module M . Therefore, it is essential to employ an effective and efficient optimization strategy that specifically generates *MICS* caused by errors in the target module, leading to system failures.

To address these challenges, we propose *MoDitector*, a Module-Directed Testing framework for Autonomous Driving Systems, designed to automatically generate *MICSs* that reveal ADS failures for different modules. *MoDitector* comprises three main components: *Module-Specific Oracle*, *Module-Specific Feedback* and *Adaptive Seed Generation*. To tackle the first challenge ❶, we design various module-specific metrics that can be used as the oracles in the ADS, allowing each module's performance to be evaluated independently. During the testing phase, *Module-Specific Oracle* can filter failures that are not caused by the errors of the target module. To address the second challenge ❷, we introduce *Module-Specific Feedback* and *Adaptive Seed Generation* to improve the optimization of detecting *MICSs*. Specifically, *Module-Specific Feedback* provides feedback that reflects the extent of errors in different modules, enabling *MoDitector* to search for *MICSs* by maximizing errors in the targeted module while minimizing errors in other modules. Furthermore, *Adaptive Seed Generation* enhances testing performance by incorporating adaptive seed selection and mutation strategies. It prioritizes seeds with higher feedback values and adaptively adjusts mutation strategies based on feedback, thereby increasing the performance of detecting *MICSs*.

We have evaluated *MoDitector* on the ADS platform Pylot [20] using the high-fidelity simulator CARLA [13]. We compared *MoDitector* with three baseline methods: *Random*, i.e., which generates scenarios randomly, along with two state-of-the-art ADS testing methods, i.e., AVFuzzer [31] and BehAVExplor [8]. The evaluation results demonstrate the effectiveness and efficiency of *MoDitector* in detecting *MICSs*, uncovering ADS failures across four different modules. For example, *MoDitector* generates a total of 55.3, 75.3, 71.7, and 14.3 *MICSs* for the perception, prediction, planning, and control modules across four testing scenarios, respectively, while the best-performing baseline detects only 18.3, 25.3, 34.3, and 7.0 *MICSs* for these modules. Further experimental results demonstrate the fidelity of the designed *Module-Specific Oracle*, the effectiveness of *Module-Specific Feedback*, and the usefulness of the *Adaptive Seed Generation* component within *MoDitector*.

In summary, this paper makes the following contributions:

- (1) To the best of our knowledge, this is the first study to investigate the generation of Module-Induced Critical Scenarios, which highlight specific weaknesses within individual modules of the ADS.
- (2) We conduct an empirical study on existing methods, revealing limitations in module-based testing for causing system failures and in system-level testing for covering weaknesses across diverse modules in the ADS.
- (3) We have developed a novel testing framework that effectively and efficiently generates *MICSs*. This framework provides fine-grained evaluation results at the module level. To assess module correctness, we have designed specific metrics that serve as oracles for various modules.
- (4) We conduct extensive experiments to evaluate the effectiveness and usefulness of *MoDitector* on Pylot. On average, 13.8, 18.8, 17.9, and 2.6 *MICSs* were discovered across four initial scenarios

for the four main modules (perception, prediction, planning, and control), demonstrating *MoDitector*'s value in detecting module-specific failures.

2 Background

2.1 Autonomous Driving System

Autonomous Driving Systems (ADSs) rely on advanced artificial intelligence algorithms as the brain of autonomous vehicles, governing their movements. ADSs can be broadly categorized into two types: End-to-End (E2E) ADSs and Module-based ADSs. E2E ADSs, such as Openpilot [2], approach the system as a single deep learning model that processes sensor data (e.g., images) as input and directly outputs control commands to operate the vehicle. The development of E2E ADSs requires vast amounts of data to achieve satisfactory performance levels, which limits their generalization capabilities and industrial-level reliability. In contrast, module-based ADSs, such as Pylot [20], Apollo [4], and Autoware [1], demonstrate more reliable performance in industrial applications by incorporating multiple modules dedicated to specific tasks. Therefore, in this paper, we focus on testing module-based ADSs to highlight critical issues arising from a specified module. Formally, we denote the module-based ADS under test as $\mathcal{A} = \{M^1, \dots, M^K\}$, where M^i represents an individual module within the ADS, and K is the total number of modules in the system. Typically, with perfect sensor data (e.g., GPS signals) and map data, module-based ADSs consist of four primary functional modules: *Perception*, *Prediction*, *Planning*, and *Control*.

Perception. The Perception module aims to detect objects (e.g., vehicles, pedestrians) surrounding the ego vehicle by processing sensor data (e.g., images, LiDAR points). Formally, at timestamp t , given sensor data \bar{I}_t , the perception module outputs a sequence of detected objects in the format of bounding boxes, represented as $\mathcal{B}_t = \{B_t^1, \dots, B_t^{N_t}\}$, where B_t^i represents the predicted bounding box of the i -th object and N_t is the number of detected objects.

Prediction. The Prediction module aims to anticipate the future movements of detected objects. Using the outputs from the *Perception* module, it predicts the trajectories of these objects over a future time horizon Δt . Formally, at timestamp t , given the detected objects \mathcal{B}_t , the prediction module outputs a sequence of future trajectories for each object, represented as $\mathcal{T}_t = \{\tau_t^1, \dots, \tau_t^{|\mathcal{B}_t|}\}$, where τ_t^i is the predicted trajectory of the i -th object, and $|\mathcal{B}_t|$ is the number of detected objects. Each trajectory $\tau_t^i = \{p_{t+k}^i \mid k = 1, \dots, H_{\text{pred}}\}$ includes a series of future waypoints over a specified prediction horizon H_{pred} , indicating the number of future timesteps for which predictions are made.

Planning. The *Planning* module is responsible for determining a safe and efficient path for the ego vehicle, considering the current road conditions and the predicted movements of surrounding objects. Based on the outputs from both the *Perception* and *Prediction* modules, it computes a trajectory for the ego vehicle that adheres to safety constraints and follows driving goals, such as reaching a destination or maintaining lane position. Formally, at timestamp t , given the detected objects \mathcal{B}_t and predicted trajectories \mathcal{T}_t , the planning module generates a planned path \mathcal{P}_t for the ego vehicle. Here, $\mathcal{P}_t = \{p_{t+k}^{\mathcal{A}} \mid k = 1, \dots, H_{\text{plan}}\}$ is a sequence of waypoints that the ego vehicle should follow over a specified planning horizon H_{plan} .

Control. The *Control* module translates the planned path from the *Planning* module into actionable control commands that adjust the ego vehicle's steering and acceleration to follow the planned trajectory. This module works at a high frequency to ensure real-time responsiveness and vehicle stability. At timestamp t , given the planned path \mathcal{P}_t , the control module generates a control command, represented as $C_t = \{C_t^{\text{steer}}, C_t^{\text{throttle}}, C_t^{\text{brake}}\}$, where C_t^{steer} , C_t^{throttle} , and C_t^{brake} represent the steering, throttle, and braking commands to be executed by the vehicle at timestamp t , respectively.

2.2 Scenario

2.2.1 Scenario Definition. In ADS testing, scenarios represent driving environments structured as sequences of scenes, each capturing a snapshot of scenery and dynamic objects. Scenarios consist of configurable static attributes (e.g., map, weather) and dynamic attributes (e.g., behaviors of NPC vehicles), derived from Operational Design Domains (ODDs) [43]. Given the vast attribute space, it is impractical to test all attribute combinations. Following previous studies [8, 31], we focus on subsets aligned with specific testing goals. In this study, our objective was to test the safety of a module-based ADS, including perception, prediction, planning, and control modules, by configuring the trajectories and weather parameters of NPC vehicles. Formally, a *scenario* can be defined as a tuple $s = \{\mathbb{A}, \mathbb{P}, \mathbb{E}\}$, where \mathbb{A} represents the ADS motion task, including the start position and destination; \mathbb{P} is a finite set of objects, encompassing static obstacles, dynamic NPC vehicles, and pedestrians; and \mathbb{E} is the set of weather parameters, such as cloudiness. For each object $P \in \mathbb{P}$, we represent its behavior with a sequence of waypoints, denoted by $W^P = \{w_1, \dots, w_n\}$. Each waypoint w_i specifies the location (x_i, y_i) and velocity v_i .

2.2.2 Scenario Observation. A scenario observation is a sequence of scenes recorded during the execution of the scenario, where each scene represents the states of the ego vehicle and other participants at a specific timestamp. Formally, given a scenario s , its observation is denoted as $O(s) = \{o_0, o_1, \dots, o_T\}$, where T is the length of the observation, and $o_t = \{\mathcal{A}_t, \mathcal{Y}_t\}$ is the scene at timestamp t , including the observation \mathcal{A}_t extracted from the ADS and \mathcal{Y}_t from the simulator. In detail, $\mathcal{Y}_t = \{y_t^{\mathcal{A}}, y_t^{P_1}, \dots, y_t^{P_{|\mathbb{P}|}}\}$ contains the states of all objects, including the ego vehicle ($y_t^{\mathcal{A}}$), where $y_t^P = \{p_t^P, b_t^P, \theta_t^P, v_t^P, a_t^P\}$ denotes the waypoint of participant $P \in \mathbb{P}$ at timestamp t . Each waypoint includes the center position p_t^P , bounding box b_t^P , heading θ_t^P , velocity v_t^P , and acceleration a_t^P . Note that the ADS observation \mathcal{A}_t contains the outputs of all ADS modules at timestamp t .

In the following content, to better distinguish between observations from the ADS and the simulator, we use $\mathcal{A}(s)$ and $\mathcal{Y}(s)$ to denote ADS observation and Simulator observation, respectively.

3 Problem Definition and Motivation

3.1 Problem Definition

This paper aims to detect Module-Induced Critical Scenarios (MICSs) for a specified module, defined as follows:

Definition 3.1 (M-Induced Critical Scenario). Given a ADS $\mathcal{A} = \{M^1, \dots, M^K\}$ that considers multiple modules as well as a target module $\mathcal{M} \in \mathcal{A}$ to be tested, the \mathcal{M} -Induced Critical Scenario s satisfies the conditions:

- a. $s \in \mathbb{S}^{Fail}$
- b. $\exists s_i \in s. error(s_i, \mathcal{M}) = True$
- c. $\forall s_i \in s. \forall \mathcal{M} \in \mathcal{A}. \mathcal{M} \neq \mathcal{M} \wedge error(s_i, \mathcal{M}) = False$

where \mathbb{S}^{Fail} denotes the set of scenarios containing ADS failures, s_i is a scene in s , and the *error* function determines whether the module \mathcal{M} exhibits errors in a specific scene. Intuitively, if we identify a critical scenario s that results in a failure, and only \mathcal{M} induces errors while all other modules operate correctly across all scenes in s , then we can conclude that the failure is primarily caused by \mathcal{M} .

Note that while failures that do not meet the MICS conditions may still be useful, they do not align with our objectives as we aim to evaluate the quality of individual modules within the ADS. Specifically, we need to accurately localize the root cause in terms of specific modules. If several modules exhibit errors in a critical scenario, it becomes challenging to conclusively determine

Table 1. Module Failures and Collision Distributions of Existing Methods

Method	$M^{\text{Perc}}\text{ICS}$	$M^{\text{Pred}}\text{ICS}$	$M^{\text{Plan}}\text{ICS}$	$M^{\text{Ctrl}}\text{ICS}$	Non-MICS
AVFuzzer	9	17	23	2	47
BehAVExplor	6	57	9	3	190

Table 2. The ratio of module errors that can cause system failures

Module	Perception			Prediction			Planning		
	10%	20%	50%	0.1m	0.5m	1m	0.1m	0.2m	0.5m
R1	0.02	0.03	0.29	0.02	0.20	0.57	0.03	0.19	0.28
R2	0.01	0.01	0.09	0.01	0.15	0.40	0.03	0.14	0.30
R3	0.07	0.09	0.18	0.01	0.15	0.39	0.04	0.11	0.34
Average	0.03	0.06	0.19	0.01	0.17	0.45	0.03	0.15	0.31

which module is the root cause. Hence, it is not a good case for developers to analyze and repair. Furthermore, based on our definition, this situation highlights our two main challenges: 1) the *error* function, which determines whether a module functions correctly, and 2) the effective method to identify *MICS* s that satisfies all necessary conditions.

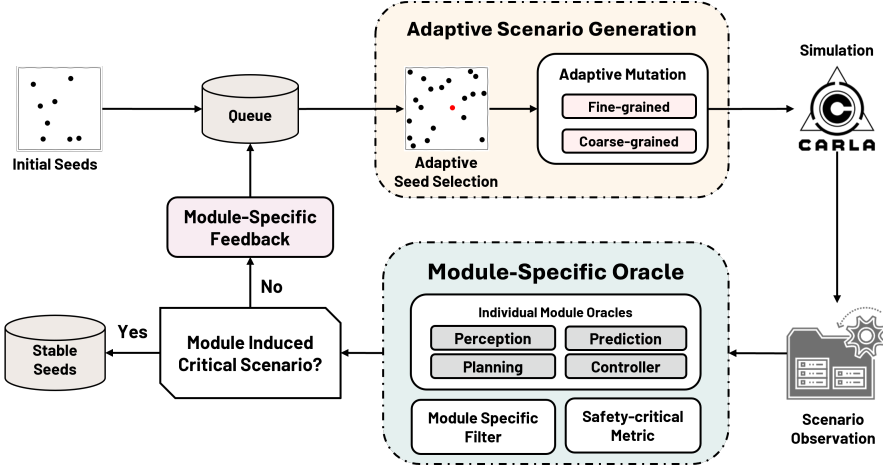
3.2 Preliminary Study

Based on the problem definition, we would like to understand the limitations of existing methods in detecting *MICS*. Specifically, both end-to-end system-level testing and module-level testing may generate failures that reveal limitations of individual modules. Therefore, we first conduct an empirical study to evaluate: 1) whether failures generated by system-level testing adequately reflect the diversity of module weaknesses, and 2) whether errors identified through module-level testing can trigger system failures.

3.2.1 The ability of existing scenario-based testing methods to generate *MICS*. Existing scenario-based methods aim to identify test scenarios that cause ADS failures efficiently but lack root cause analysis for module errors. To explore the capabilities of existing methods in generating *MICS*, we conducted experiments using two scenario-based testing scenario generation methods, AVFuzzer[31] and BehAVExplor[8]. In these experiments, we utilized Pylot[20] as the tested ADS and CARLA as the simulator. Starting with four basic scenarios (detailed in Section 5), each method was run for 6 hours, and we recorded the module errors and *MICS* collected during this period.

The results shown in table 1 of these two existing works show high similarity. They generate many collisions, however, most are non-*MICS*, in which multiple modules typically experience errors before a collision occurs. On the other hand, though some *MICS* have been generated, the distribution is highly uneven, with most *MICS* introduced by the prediction module, while *MICS* from other modules are rare. This imbalance makes it challenging for developers to improve the corresponding modules effectively.

3.2.2 Limitation on module-level evaluation for ADS testing. To better investigate the relationship between module-level errors and system-level failures in ADS, we manually introduced random noise to the output of the perception, prediction and planning module since the results in table 1 tend to be error-prone. For the perception module, we applied one of three operations—*Zoom In*, *Zoom Out*, and *Random Offset*—randomly to each bounding box. For the prediction and planning modules, we added random perturbations to trajectory nodes. For each module, we established three levels of random error limits: conventional, moderate, and extreme. The specific settings are as follows: • Perception: [10%, 20%, 50%]; • Prediction: [0.1m, 0.5m, 1m]; • Planning: [0.1m, 0.2m, 0.5m]. We randomly selected 100 normal running scenarios from 3.2.1, with each experiment

Fig. 1. Overview of *MoDetector*

only perturbing one module’s output. To mitigate the effects of randomness, each experiment was repeated three times.

Table 2 shows the results of operations after introducing manual injections. As the results show, aside from experiments with extreme perturbations (the third column for each module), the module errors alone does not effectively lead to system-level failures. With conventional-level perturbations to module outputs, only a few running failures occurred; even with moderate-level perturbations, the failure rate reached only up to 17%. This suggests a significant gap between module-level errors and system failures, indicating the need for a mapping method to rapidly identify the corresponding MICSs and bridge this gap effectively.

Motivation: Existing system-level and module-level testing methods failed to generate MICSs. This limitation motivates us to develop an effective approach to detecting system failures induced by specified modules.

4 Approach

4.1 Overview

Fig. 1 provides a high-level overview of *MoDetector* for generating MICSs given initial seeds and the user-specified module M . *MoDetector* comprises three main components: *Module-Specific Oracle*, *Module-Specific Feedback* and *Adaptive Seed Generation*. *Module-Specific Oracle* functions as an oracle to check whether a scenario satisfies Definition 3.1 and qualifies as an MICS. *Module-Specific Feedback* provides feedback that guides the search process, which jointly considers the system-level specifications (i.e., safety) and the module-specific aspects (i.e., the extent of errors in M). *Adaptive Seed Generation* implements an adaptive strategy, including seed selection and mutation, to generate new scenarios based on the module-specific feedback score, thereby improving search performance. Specifically, following a classical search-based fuzzing approach, *MoDetector* maintains a seed corpus with valuable seeds that facilitate the identification of MICSs. In each iteration, *Adaptive Seed Generation* first chooses a seed with a higher feedback score and applies an adaptive mutation to the selected seed to generate a new test scenario. Note that a higher feedback score indicates

Algorithm 1: Workflow of *MoDitector*

Input : Initial seed corpus \mathbf{Q}
 ADS under test $\mathcal{A} = \{M^1, \dots, M^K\}$
 Specified module $\mathcal{M} \in \mathcal{A}$

Output : \mathcal{M} module-induced critical scenarios $\mathbf{F}_{\mathcal{M}}$

```

1  $\mathbf{F}_{\mathcal{M}} \leftarrow \{\}$ 
2 repeat
3    $s', \phi_s \leftarrow \text{AdaptiveScenariGeneration}(\mathbf{Q})$  // Generate new scenarios
4    $\mathcal{O}(s') = \{\mathcal{A}(s'), \mathcal{Y}(s')\} \leftarrow \text{Simulator}(s', \mathcal{A})$ 
5    $r_{\mathcal{M}}, \delta^{\mathcal{A}}, \delta^{\text{safe}} \leftarrow \text{ModuleSpecificOracle}(\mathcal{A}(s'), \mathcal{Y}(s'), \mathcal{M}^k)$  // Analyze module errors
6   if  $r_{\mathcal{M}}$  is Fail then
7     // Update failure sets
8      $\mathbf{F}_{\mathcal{M}} \leftarrow \mathbf{F}_{\mathcal{M}} \cup \{s'\}$  // Update discovered MICSS
9   else
10    // Update seed corpus
11     $\phi_{s'} \leftarrow \text{ModuleSpecificFeedback}(\delta^{\text{safe}}, \delta^{\mathcal{A}})$  // Calculate feedback score
12    if  $\phi_{s'} > \phi_s$  then
13       $\mathbf{Q} \leftarrow \mathbf{Q} \cup \{s'\}$  // Update corpus for MICSS search
14 until given time budget expires;
15 return  $\mathbf{F}_{\mathcal{M}}$ 

```

a greater likelihood of evolving into an MICS. Then, *Module-Specific Oracle* and *Module-Specific Feedback* provide the identification result and feedback score for the new seed by analyzing the scenario observation, respectively.

Algorithm 1 presents the main algorithm of *MoDitector*. The algorithm takes as input an initial seed corpus \mathbf{Q} , a module-based ADS $\mathcal{A} = \{M^1, \dots, M^K\}$, which consists of K modules, and the user-specified module \mathcal{M} under test. The output is a set of module \mathcal{M} caused critical scenarios s (Line 13). In detail, *MoDitector* begins by initializing an empty set for $\mathbf{F}_{\mathcal{M}}$ (Line 1). Then *MoDitector* starts the fuzzing process, which continues until the given budget expires (lines 2-12). In each iteration, *MoDitector* first uses *Adaptive Seed Generation* to return a new scenario s' and the feedback score ϕ_s of its source seed s (Line 3). This new scenario s' is executed in the simulator with the ADS under test \mathcal{A} , collecting the scenario observation $\mathcal{O}(s') = \{\mathcal{A}(s'), \mathcal{Y}(s')\}$ including the ADS observation $\mathcal{O}_{\mathcal{A}}(s')$ and the Simulator observation $\mathcal{Y}_{\mathcal{A}}(s')$ (Line 4). Based on these observations, *Module-Specific Oracle* identifies if the scenario s' contains system failures and if module \mathcal{M}^k is the root cause, returning the identification result $r_{\mathcal{M}}$, module errors $\delta^{\mathcal{A}}$ and safety-critical distance $\delta^{\mathcal{A}}$ (Line 5). If $r_{\mathcal{M}}$ is identified as *Fail*, *MoDitector* keeps the scenario s' in the critical scenario set $\mathbf{F}_{\mathcal{M}}$ (Line 6-7). Otherwise, *Module-Specific Feedback* calculates a feedback score for the benign scenario s' based on the module errors $\delta^{\mathcal{A}}$ and the safety-critical distance δ^{safe} (Lines 8-9). A higher feedback score $\phi_{s'}$ indicates a higher potential of s' for generating MICSS. If the feedback score of seed s' is higher than that of its parent seed s , *MoDitector* retains s' in the corpus \mathbf{Q} for further optimization (Line 10-11). Finally, the algorithm ends by returning $\mathbf{F}_{\mathcal{M}}$ (Line 13).

4.2 Module-Specific Oracle

The purpose of *Module-Specific Oracle* is to serve as an oracle for automatically detecting MICSS by determining whether a given scenario satisfies all conditions outlined in *Definition 3.1*. This

involves two parts: (1) detecting system failures in the scenario (*Definition 3.1.a*) and (2) determining errors for each module in the ADS (*Definition 3.1.b* and *Definition 3.1.c*).

For part (1), we consider the occurrence of collisions as a safety-critical metric to identify system failures. For part (2), the main challenge is obtaining ground truth to evaluate the performance of individual modules without human annotation. To address this, we design *Individual Module Metrics* to independently measure errors for each module using collected scenario observations, covering the four main modules in the ADS: perception, prediction, planning, and control.

4.2.1 Safety-critical Metric. We check if the scenario contains ADS failures by detecting collisions. Specifically, we first calculate the minimum distance between the ego vehicle and other objects:

$$\delta_s^{\text{safe}} = \min \{ \|R_{\text{bbox}}(p_t^0) - R_{\text{bbox}}(p_t^n)\|_2 \mid t \in [0, T], n \neq 0 \} \quad (1)$$

where p_t^0 represents the position of the ego vehicle at time t , $R_{\text{bbox}}(\cdot)$ calculates the bounding box for an object based on its position p , and p_t^n represents the position of the n -th object at the same time. Therefore, safety-critical failures can be detected if $\delta_s^{\text{safe}} = 0$.

4.2.2 Individual Module Oracles. Given a scenario s with its observation $\mathcal{O}(s) = \{\mathcal{A}(s), \mathcal{Y}(s)\}$, we first design individual metrics for each module to measure module-level errors $\delta^M = \{\delta_t^M \mid t \in [0, \dots, T]\}$ for each module $M \in \mathcal{A}$, where δ_t^M denotes the module error at timestamp t and T is the termination timestamp of the scenario s . We detail the calculation of δ_t^M covering the *Perception*, *Prediction*, *Planning*, and *Control* modules as follows:

(1) *Perception Module.* Given a scenario s , the error in the *Perception* module can be directly measured by comparing object bounding boxes between Simulator observation $\mathcal{Y}(s)$ and ADS observations $\mathcal{A}(s)$. We adopt a weighted Intersection over Union (IoU) [19] to measure the errors in the perception module $\mathcal{M}^{\text{perc}}$, which is a widely recognized metric in object detection. Specifically, the errors of the perception module at timestamp t is calculated as follows:

$$\delta_t^{\text{perc}} = 1 - \frac{1}{N_t} \sum_{n=1}^{N_t} \left(\frac{D - d_t^n}{D} \cdot \frac{|B_t^n \cap b_t^n|}{|B_t^n \cup b_t^n|} \right) \quad (2)$$

where N_t represents the number of detected objects within the perception range D meters, B_t^n and b_t^n denote the detected bounding box and the ground truth bounding box of the n -th object, respectively, obtained from the ADS observation $\mathcal{A}_t \in \mathcal{A}(s)$ and the scenario observation $\mathcal{Y}_t \in \mathcal{Y}(s)$. The weight $\frac{D - d_t^n}{D}$ assigns a higher weight to objects closer to the ego vehicle, where d_t^n denotes the distance between the n -th object and the ego vehicle at timestamp t . A higher value of δ^{perc} represents a greater detection error in the perception module, indicating a potential safety-critical situation.

(2) *Prediction Module.* Unlike the *Perception* module, directly comparing the predicted trajectories in ADS observation $\mathcal{A}(s)$ with the collected trajectories in Simulator observation $\mathcal{Y}(s)$ cannot accurately reflect errors in the *Perception* module. This is because the inputs to the *Prediction* module are derived from the *Perception* module, which may introduce perception errors that subsequently affect prediction outcomes. To address this, we adopt a perception-biased trajectory to measure the errors in the *Prediction* module. Specifically, at timestamp t , the perception-biased trajectory for the n -th object within perception range D is determined by incorporating the biases present in the perception module, formulated as:

$$\bar{\tau}_t^n = \{ p_{t+k}^n + \Delta p_t^n \mid k \in [0, \dots, H_{\text{pred}}] \} \quad (3)$$

where p_{t+k}^n represents the ground-truth position in the Simulator observation \mathcal{Y}_t , and Δp_{t+k}^n is the position shift observed in the *Perception* module, and H_{pred} is the prediction horizon. Note that the position shift $\Delta p_t^n = (\Delta x_t^n, \Delta y_t^n)$ represents the positional difference between the detected output and the ground truth at timestamp t . Since the following detect output after timestamp t is

unavailable, and the offset does not fluctuate significantly within a shorter prediction window (about 0.5 to 1 seconds) in most cases, we apply Δp_t^n to its predicted sequence.

Consequently, we can measure the error of the *Prediction* module by comparing the predicted trajectories with the perception-biased trajectories. This comparison is quantified by:

$$\delta_t^{\text{pred}} = \max \left\{ \frac{D - d_t^n}{D} \cdot \|\hat{p}_{t+k}^n - \bar{p}_{t+k}^n\|_2 \mid \hat{p}_{t+k}^n \in \tau_t^n, \bar{p}_{t+k}^n \in \bar{\tau}_t^n, n \in [1, \dots, N_t] \right\} \quad (4)$$

where N_t is the number of detected objects within the perception range D , τ_t^n is the predicted trajectory for the n -th object, and d_t^n denotes the distance between the n -th object and the ego vehicle at timestamp t . The calculation of δ_t^{pred} selects the maximum error in all predicted trajectories because this emphasizes the worst-case performance within a given scenario, which is crucial for assessing the robustness and safety of the *Prediction* module.

(3) *Planning Module*. We measure errors in the *Planning* module from a safety perspective by evaluating the distance to collisions. Similar to the prediction module, biases present in upstream modules (i.e., *Perception* and *Prediction*) affect the evaluation of the planning module when directly using ground truth data collected from the Simulator observation $\mathcal{Y}(s)$. To mitigate these biases, we measure errors in the *Planning* module by assessing if the planned trajectories collide with objects detected by the upstream modules. This is calculated by:

$$\delta_t^{\text{plan}} = \sum_{n=1}^{N_t} \sum_{k=1}^{H_{\text{plan}}} \mathbb{I}(\|R_{\text{bbox}}(p_{t+k}^{\mathcal{A}}) - R_{\text{bbox}}(p_{t+k}^n)\|_2 = 0) \quad (5)$$

where N_t represents the number of detected objects, H_{plan} is the planning horizon, $R_{\text{bbox}}(\cdot)$ calculates the bounding box for an object based on its position p , $\mathbb{I}(\cdot)$ is an indicator function. The indicator function $\mathbb{I}(\text{condition})$ returns 1 if the *condition* is true and 0 otherwise. Additionally, $p_{t+k}^{\mathcal{A}} \in \mathcal{P}_t$ denotes a trajectory point planned by the *Planning* module, and $p_{t+k}^n \in \tau_t^n$ is the predicted trajectory point for the n -th object at timestamp t . Ideally, the planned trajectory should be collision-free, maintaining a safety distance from all predicted states of all objects (i.e., $\delta_t^{\text{plan}} = 0$). Therefore, a larger δ_t^{plan} indicates that the planning module has safety-critical errors, such as collisions.

(4) *Control Module*. The control command is directly applied to the vehicle to manage its movement by following a trajectory from the upstream *Planning* module. Obtaining a ground truth for control commands is challenging. Thus, we evaluate the *Control* module by comparing the actual movement of the vehicle with the planned movement from the *Planning* module. At timestamp t , we calculate the error for the *Control* module by:

$$\delta_t^{\text{ctrl}} = \|p_{t+1}^{\mathcal{A}} - p_{t+1}^0\|_2 + \|v_{t+1}^{\mathcal{A}} - v_{t+1}^0\|_2 \quad (6)$$

where $p_{t+1}^{\mathcal{A}}$ and $v_{t+1}^{\mathcal{A}}$ represent the planned position and velocity from the *Planning* module at timestamp t , and p_{t+1}^0 and v_{t+1}^0 are the actual position and velocity of the vehicle at timestamp $t + 1$. This error δ_t^{ctrl} quantifies how well the *Control* module is executing the planned trajectory. A larger error value indicates a significant deviation from the planned path and speed, suggesting potential issues in the *Control* module (i.e., inaccuracies in executing the planned trajectory).

4.2.3 Module-Specific Filter. The Module-Specific Filter aims to filter out less relevant module errors, as driving scenes farther from the termination have less impact on the final results [40, 41]. The filter considers only module errors within a detection window $[T - \Delta t, T]$, where T is the timestamp of the occurrence of system failures in the scenario, and Δt is the detection window size.

Algorithm 2: Algorithm for *Module-Specific Oracle*

Input : Scenario observation $O(s) = \{\mathcal{A}(s), \mathcal{Y}(s)\}$
 ADS $\mathcal{A} = \{M^1, \dots, M^K\}$
 User-specified module \mathcal{M}

Output : MICS identification result $r_{\mathcal{M}}$
 Module errors $\delta^{\mathcal{A}} = \{\delta^{M^1}, \dots, \delta^{M^K}\}$
 Safety-critical distance δ^{safe}

```

1  $\delta^{\mathcal{A}} \leftarrow \{\}, r_{\mathcal{M}} \leftarrow \text{Pass}$ 
2  $\delta^{\text{safe}} \leftarrow$  calculate safety-critical distance by Eq. 1( $\mathcal{Y}(s)$ ) // Safety-critical metric
3 if  $\delta^{\text{safe}} \neq 0$  then
4    $r_{\mathcal{M}} \leftarrow \text{Fail}$  // Fail to satisfy Definition 3.1.a
5 for  $M$  in  $\mathcal{A}$  do
6   // Module error calculated by Individual Module Metrics
7    $\delta^M \leftarrow$  calculate the module-level error according to Section 4.2.2
8    $\hat{\delta}^M \leftarrow$  filter module errors by Eq. 7
9    $\delta^{\mathcal{A}} \leftarrow \delta^{\mathcal{A}} \cup \{\delta^M\}$ 
10  // Definition 3.1.b
11  if  $M = \mathcal{M}$  and  $\hat{\delta}^M = 0$  then
12     $r_{\mathcal{M}} \leftarrow \text{Fail}$ 
13  // Definition 3.1.c
14  if  $M \neq \mathcal{M}$  and  $\hat{\delta}^M \neq 0$  then
15     $r_{\mathcal{M}} \leftarrow \text{Fail}$ 
16 return  $r_{\mathcal{M}}, \delta^{\mathcal{A}}, \delta^{\text{safe}}$ 

```

Therefore, the filtered module errors are calculated by:

$$\hat{\delta}^M = \sum_{t=T-\Delta t}^T \mathbb{I}(\delta_t^M > \lambda^M) \quad (7)$$

where λ^M is the tolerance threshold for module M , and \mathbb{I} is an indicator function. The indicator function $\mathbb{I}(\text{condition})$ returns 1 if the *condition* is true and 0 otherwise.

4.2.4 Workflow of Module-Specific Oracle. Algorithm 2 illustrates the workflow of *Module-Specific Oracle*. Specifically, the algorithm takes as inputs the scenario observation $O(s)$, the ADS \mathcal{A} , and the user-specified module \mathcal{M} , and it outputs three key results: the identification result $r_{\mathcal{M}}$, the module errors's set $\delta^{\mathcal{A}}$, the safety-critical distance δ^{safe} . Initially, *Module-Specific Oracle* creates an empty error set $\delta^{\mathcal{A}}$ to store module errors and an identification flag $r_{\mathcal{M}}$ set to 'pass' (Line 1). Then, the algorithm calculates the safety-critical distance using Eq. 1 and checks for system failures (Lines 2-4), aiming to confirm the satisfaction of *Definition 3.1.a*. Subsequently, the algorithm calculates and filters module errors for each module in the ADS \mathcal{A} , storing these errors in $\delta^{\mathcal{A}}$ for further analysis and feedback (Lines 5-8). Once the user-specified module does not trigger errors (Line 9-10) or other modules do trigger errors (Line 11-12), the identification flag is set to 'Fail' as they violate the requirements of *Definition 3.1.b* and *Definition 3.1.c*. Finally, *Module-Specific Oracle* returns the identification flag $r_{\mathcal{M}}$, the module error set $\delta^{\mathcal{A}}$, and the safety-critical distance δ^{safe} (Line 13).

4.3 Module-Specific Feedback

To provide guidance for searching MICSs, we design a *Module-Specific Feedback* providing a feedback score, including two parts: (1) *safety-critical score* and (2) *module-directed score*. The *safety-critical score* aims to guide the search for safety-critical scenarios that include system-level violations (i.e., collisions). To focus more specifically on the user-specified module, we introduce the *module-directed score*, which provides guidance to bias the generation of safety-critical scenarios towards this module.

4.3.1 Safety-critical Score. We directly leverage the safety-critical distance from Section 4.2.1 as our safety-critical feedback score, denoted by $\phi_s^{\text{safe}} = \delta_s^{\text{safe}}$. The safety-critical score ϕ_s^{safe} quantifies the minimum distance between the ego vehicle and other objects over the time horizon $[0, T]$, capturing how close the vehicle comes to a collision scenario. A lower value of ϕ_s^{safe} indicates a more dangerous situation for the ego vehicle.

4.3.2 Module-directed Score. Given a user-specified module \mathcal{M} , we calculate the *module-directed score* as follows:

$$\phi_s^{\mathcal{M}} = \sum_{t=T-\Delta t}^T \left(\delta_t^{\mathcal{M}} - \frac{\sum_{M \neq \mathcal{M}} \delta_t^M}{K-1} \right) \quad (8)$$

where K is the total number of modules in the ADS \mathcal{A} , T is the termination timestamp of scenario s , Δt is the detection window, and δ_t^M represents the module-level errors for each module obtained from *Module-Specific Oracle*, as detailed in Section 4.2.2. The first term, $\delta_t^{\mathcal{M}}$, quantifies the errors specific to the user-specified module \mathcal{M} . The second term, $\frac{\sum_{M \neq \mathcal{M}} \delta_t^M}{K-1}$, represents the average of the cumulative errors across all other modules. The score $\phi_s^{\mathcal{M}}$ promotes the search for scenarios in which only the user-specified module \mathcal{M} exhibits errors during the detection window, while other modules do not. Therefore, this score can provide guidance to enhance the impact of the user-specified module \mathcal{M} on detected violations.

The final feedback score combines the *safety-critical score* and the *module-directed score* by:

$$\phi_s = \phi_s^{\mathcal{M}^k} - \phi_s^{\text{safe}} \quad (9)$$

A larger ϕ_s indicates that the scenario s is closer to becoming a MICS. Consequently, *MoDitector* aims to generate MICSs by maximizing this feedback score.

4.4 Adaptive Scenario Generation

To improve the searching performance of *MoDitector*, we design an *Adaptive Seed Generation* mechanism including *Adaptive Seed Selection* and *Adaptive Mutation*, which adaptively generate new seed scenarios based on the feedback score obtained from *Module-Specific Feedback*.

4.4.1 Adaptive Seed Selection. The seed selection process aims to choose a seed scenario from the seed corpus for further mutation, thereby generating a new scenario. We design this selection process to favor seeds with higher feedback scores, indicating they are more likely to evolve into a MICS. Therefore, we assign a selection probability to each seed in the corpus based on the feedback score calculated by *Module-Specific Feedback*. The selection probability for each seed s is defined as:

$$p(s) = \frac{\phi_s - \phi_{\min} + \epsilon}{\sum_{s' \in \mathcal{Q}} (\phi_{s'} - \phi_{\min} + \epsilon)} \quad (10)$$

where ϕ_{\min} is the global minimum feedback score in the corpus, ϕ_s is the feedback score for seed s , ϵ is a small positive constant to ensure that the seed with the global minimum feedback score has a non-zero selection probability, and \mathcal{Q} denotes the set of all seeds in the corpus. This probability

Algorithm 3: Algorithm for *Adaptive Mutation*

```

Input      : Selected seed  $s$  with feedback score  $\phi_s$ 
              Maximum feedback score  $\phi_{max}$  and Minimum feedback score  $\phi_{min}$  in the seed corpus
Output    : Mutated seed  $s'$ 
1  $s' \leftarrow s$  // Copy the selected scenario seed  $s$ 
2  $\lambda_m \leftarrow \frac{\phi_{max} - \phi_s}{|\phi_{max} - \phi_{min}|}$  // Assign a dynamic threshold for determining mutation strategy
3 if  $random() > \lambda_m$  then
  // Fine-grained mutation: add small perturbation
4    $\mathbb{E}_{s'} \leftarrow \mathbb{E}_{s'} + \text{GaussSample}(\lambda_m)$ 
5   for  $P \in \mathbb{P}_{s'}$  do
6      $W_P^v \leftarrow W_P^v + \text{GaussSample}(\lambda_m)$ 
7 else
  // Coarse-grained mutation: regenerate new parameters
8    $\mathbb{E}_{s'} \leftarrow \text{UniformSample}([\mathbb{E}_{min}, \mathbb{E}_{max}])$ 
9   for  $P \in \mathbb{P}_{s'}$  do
10     $W_P^l \leftarrow \text{RouteGenerate}(\lambda_m)$ 
11     $W_P^v \leftarrow \text{UniformSample}([V_{min}, V_{max}], \lambda_m)$ 
12 return  $s'$ 

```

formulation ensures that seeds with higher feedback scores have a higher chance of being selected for mutation, thereby promoting the generation of scenarios with a higher likelihood of evolving into a MICs.

4.4.2 Adaptive Mutation. Beyond seed selection, we also design an adaptive mutation strategy that applies different mutation methods based on the feedback score of each seed. Algorithm 3 presents the details of *Adaptive Mutation*. Specifically, given a scenario s , the *Adaptive Mutator* first copies the source seed s to s' (Line 1) and calculates a dynamic threshold $\lambda_m = \frac{\phi_{max} - \phi_s}{|\phi_{max} - \phi_{min}|} \in [0, 1]$ by normalizing the feedback score ϕ_s , ensuring λ_m (Line 2). Then, the mutation selects either *fine-grained mutation* or *coarse-grained mutation* based on the derived dynamic threshold λ_m (Line 3-11). Seeds with higher feedback scores (resulting in smaller dynamic thresholds) are regarded as closer to MICs; therefore, we employ *fine-grained mutation* to add Gaussian noise to the weather parameters (Line 4) and the speeds of each object (Lines 5-6). Otherwise, for seeds with lower feedback scores (resulting in larger dynamic thresholds), we utilize *coarse-grained mutation* to introduce more significant variations. These include changing the trajectory waypoints of each object and altering environmental conditions through uniform sampling (Lines 7-11). Finally, a mutated scenario s' is produced (Line 12).

5 Evaluation

In this section, we aim to empirically evaluate the effectiveness of *MoDitecor* in generating MICs. Specifically, we will address the following research questions:

RQ1: Can *MoDitecor* effectively generate MICs across different modules of the ADS?

RQ2: How accurate is *Module-Specific Oracle* in identifying MICs?

RQ3: What is the usefulness of *Module-Specific Feedback* and *Adaptive Seed Generation* in *MoDitecor*?

RQ4: How does *MoDitecor* perform from the perspective of testing efficiency?

To address these research questions, we conducted experiments using the following settings:

Table 3. Comparison results with baselines.

Method	# $\mathcal{M}^{\text{perc}}$					# $\mathcal{M}^{\text{pred}}$					# $\mathcal{M}^{\text{plan}}$					# $\mathcal{M}^{\text{ctrl}}$				
	S1	S2	S3	S4	Sum.	S1	S2	S3	S4	Sum.	S1	S2	S3	S4	Sum.	S1	S2	S3	S4	Sum.
<i>Random</i>	2.3	1.7	2.0	1.7	7.7	6.3	11.3	4.0	1.7	23.3	11.3	11.7	7.3	3.7	34.0	3.3	0	1.3	0	4.6
<i>AVFuzzer</i>	3.3	4.7	1.3	3.7	13.0	11.7	6.7	3.7	3.3	25.3	7.7	10.7	5.7	5.3	29.3	3.7	0.7	2.0	0.3	6.7
<i>BehAVExplor</i>	5.3	4.3	4.3	5.7	18.3	6.7	10.3	6.0	1.3	19.3	11.0	13.3	7.3	2.7	34.3	4.7	1.3	1.0	0.0	7.0
<i>MoDitector</i>	23.0	7.7	14.0	10.7	55.3	28.7	24.3	13.3	9.0	75.3	26.0	21.0	18.0	6.7	71.7	6.0	5.0	2.0	1.3	14.3

Environment. We conducted our experiments using Pylot [20] and CARLA [13]. Pylot, a widely popular open-source, multi-module ADS platform, includes modules for Perception $\mathcal{M}^{\text{perc}}$, Prediction $\mathcal{M}^{\text{pred}}$, Planning $\mathcal{M}^{\text{plan}}$, and Control $\mathcal{M}^{\text{ctrl}}$. CARLA is a high-fidelity simulator that is compatible with Pylot.

Driving Scenarios. We evaluate *MoDitector* on four representative scenarios derived from the NHTSA pre-crash typology [35], which is also widely utilized in existing ADS testing techniques [8, 31]. Specifically, these scenarios are:

S1: The ego vehicle starts in a weave zone and merges onto the highway.

S2: The ego vehicle leaves the highway via an exit ramp.

S3: The ego vehicle turns left at an uncontrolled intersection.

S4: The ego vehicle turns right at an uncontrolled intersection; a full stop is required before turning.

Baselines. We selected three state-of-the-art system-level testing methods for the comparisons. We first select a *Random* method that randomly generates scenarios. Additionally, we included two representative state-of-the-art ADS testing techniques for reference: *AVFuzzer* [31] and *BehAVExplor* [8]. *AVFuzzer* aims to efficiently identify collisions, whereas *BehAVExplor* focuses on discovering a more diverse set of safety-critical scenarios. Note that *AVFuzzer* and *BehAVExplor* were originally evaluated using the Apollo [4] with LGSVL [38]. However, since LGSVL was sunsetted in 2022 [30], we adapted these techniques to our simulation environment, Pylot with CARLA, for comparison.

Metrics. To evaluate the effectiveness of *MoDitector*, we utilize the metric $\#\mathcal{M}^k$, which quantifies the number of generated MICSs for the user-specific module \mathcal{M}^k . Additionally, we aim to confirm that the detected MICSs are truly induced solely by errors in the module \mathcal{M} . To this end, we define a repair rate metric as $\%\mathcal{M}^k = \frac{\#\mathcal{M}_{\text{rep}}^k}{\#\mathcal{M}^k} \times 100\%$ to verify the correctness of *Module-Specific Oracle*, where $\#\mathcal{M}_{\text{rep}}^k$ denotes the number of MICSs successfully repaired. Here, k is the identifier for the module \mathcal{M}^k ; for instance, $k = \text{perc}$ denotes the Perception module. Specifically, we rerun and repair the detected MICS by replacing the outputs of \mathcal{M}^k with the ground truth. Subsequently, we count the number of MICS that have been repaired and no longer present any safety-critical issues.

Implementation. According to our preliminary study (see Section 3.2), we set the tolerance thresholds $\lambda_{\mathcal{M}^k}$ for Perception, Prediction, and Control modules as $\lambda_{\mathcal{M}^{\text{perc}}} = 0.5$, $\lambda_{\mathcal{M}^{\text{pred}}} = 0.1$, $\lambda_{\mathcal{M}^{\text{plan}}} = 0$, and $\lambda_{\mathcal{M}^{\text{ctrl}}} = 0.05$, respectively. The detection window size Δt is set to 0.5 seconds because this is the smaller length of the prediction and planning module output in Pylot’s default configuration. In our experiments, we utilize the synchronized mode in CARLA to mitigate the influence of non-determinism inherent in the simulation-based execution of the ADS. We repeat each experiment three times with different random seeds to report the average of the results. For each run, we use a consistent budget of three hours, which we found sufficient for comparison.

5.1 RQ1: Effectiveness of *MoDitector*

5.1.1 Comparative Results. Table 3 presents the comparison results on the number of generated MICS $\#\mathcal{M}^k$, for each individual module in the ADS, covering Perception $\#\mathcal{M}^{\text{perc}}$, Prediction $\#\mathcal{M}^{\text{pred}}$,

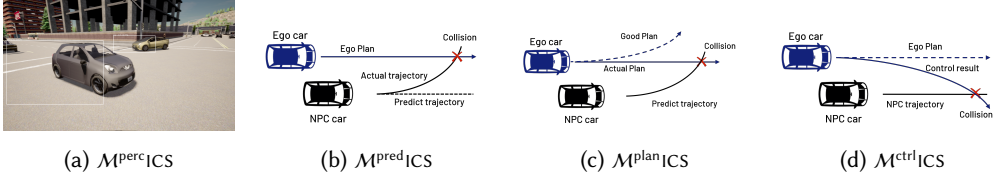


Fig. 2. Cases of MICs detected by *MoDetector* for different specific modules.

Planning $\#M^{\text{plan}}$, and Control $\#M^{\text{ctrl}}$. From the results, we can find that *MoDetector* achieves significantly better performance than other baselines in generating MICs for each module. Specifically, in terms of the *Sum.* numbers of $\#M^k$, *MoDetector* substantially outperforms the best baseline: *BehAVExplor* on $\#M^{\text{perc}}$ (55.3 vs. 18.3), *AVFuzzer* on $\#M^{\text{pred}}$ (75.3 vs. 25.3), *BehAVExplor* on $\#M^{\text{plan}}$ (71.7 vs. 34.3), and *BehAVExplor* on $\#M^{\text{ctrl}}$ (6.0 vs. 4.7). It is worth noting that *BehAVExplor* outperforms other baselines in most modules due to its diversity feedback mechanism. This mechanism encourages the ego vehicle to explore different behaviors, making it more likely to generate safety-critical scenarios caused by different modules. By comparing results across different modules, we find that *MoDetector* identifies $\#M^{\text{ICS}}$ in descending order: Prediction (75.3) > Planning (71.7) > Perception (55.3) > Control (14.3). This hierarchy indicates that in the ADS, the robustness of the Prediction, Planning, and Perception modules is comparatively lower and requires further development. We note that both comparison methods and *MoDetector* only detects a very small number of $\#M^{\text{ctrl}}$. In the experiment, the control module is based on PID [26], and with appropriate parameter settings, PID controllers generally exhibit high robustness [3]. On the other hand, scenario-based testing cannot directly generate sudden load changes and other variations commonly encountered in PID testing [6]. Nonetheless, *MoDetector* still achieves an improvement over baseline methods in detecting $M^{\text{ctrl}}\text{CCS}$. Moreover, *MoDetector* consistently achieves better performance than all baselines across the four scenarios, *S1* to *S4*, demonstrating its generalization capability in various situations.

5.1.2 Case Study. Fig. 2 presents four representative MICs examples for modules in the ADS, respectively.

(a) $M^{\text{perc}}\text{ICS}$. Fig. 2(a) illustrates a collision caused solely by the Perception module. In this scenario, the ego car turns left and erroneously detects the NPC cars' locations as they shift to the left. As a result, the ADS assumes a safe distance between the detected NPC cars and, therefore, maintains its acceleration decision, ultimately leading to a collision.

(b) $M^{\text{pred}}\text{ICS}$. Fig. 2(b) illustrates a collision scenario resulting from inaccurate predictions of surrounding NPC cars' movements by the Prediction module. In this instance, the ego car maintains its lane, while a nearby NPC car on the right initiates a lane change to cut in. However, the Prediction module erroneously predicts that the NPC car will stay in its current lane. Consequently, the ADS continues its original trajectory without accounting for the NPC car's lane change, which ultimately leads to a collision.

(c) $M^{\text{plan}}\text{ICS}$. Fig. 2(c) illustrates a collision caused by the Planning module of the ego car making an unsafe decision. In this case, the ego car proceeds along its initially planned path (Actual Plan), even though a safer alternative trajectory (Good Plan) is available. The ego car fails to account for the NPC car's predicted trajectory, which leads to a close interaction. By not choosing the safer path, the Planning module's decision ultimately results in a collision with the NPC car.

(d) $M^{\text{ctrl}}\text{ICS}$. Fig. 2(d) is a collision caused by the Control module in the ADS. Specifically, the ego of the upstream Planning makes a safe planning path (Ego Plan), while the Control module can

Table 4. Correctness of *Module-Specific Oracle* for the Perception and Prediction modules.

Scenario	Perception			Prediction			Planning			Control		
	# $\mathcal{M}^{\text{perc}}$	# $\mathcal{M}_{\text{rep}}^{\text{perc}}$	% $\mathcal{M}^{\text{perc}}$	# $\mathcal{M}^{\text{pred}}$	# $\mathcal{M}_{\text{rep}}^{\text{pred}}$	% $\mathcal{M}^{\text{pred}}$	# $\mathcal{M}^{\text{plan}}$	# $\mathcal{M}_{\text{rep}}^{\text{plan}}$	% $\mathcal{M}^{\text{plan}}$	# $\mathcal{M}^{\text{ctrl}}$	# $\mathcal{M}_{\text{rep}}^{\text{ctrl}}$	% $\mathcal{M}^{\text{ctrl}}$
<i>S1</i>	23.0	21.0	91.3%	28.7	24.3	85.0%	26.0	26.0	100.0%	6.0	6.0	100.0%
<i>S2</i>	7.7	7.3	96.1%	24.3	22.0	90.5%	21.0	21.0	100.0%	5.0	5.0	100.0%
<i>S3</i>	14.0	11.7	83.6%	13.3	12.7	95.5%	18.0	18.0	100.0%	2.0	2.0	100.0%
<i>S4</i>	10.7	9.3	87.7%	9.0	8.3	92.2%	6.7	6.7	100.0%	1.3	1.3	100.0%
<i>Sum.</i>	55.3	49.3	89.2%	75.3	67.3	89.3%	71.7	71.7	100.0%	14.3	14.3	100.0%

not adjust the ego-motion according to the Ego Plan in time. The latency response in the Control module finally results in a collision with the NPC car.

Answer to RQ1: *MoDitector* can effectively generate MICs for user-specified module \mathcal{M}^k in the ADS, covering Perception, Prediction, Planning and Control modules.

5.2 RQ2: Correctness of *Module-Specific Oracle*

5.2.1 Setup. To evaluate the fidelity of *Module-Specific Oracle*, we rerun all detected MICs by substituting the outputs of module \mathcal{M}^k with perfect outputs starting from timestamp $t_{\mathcal{M}^k}$. Here, $t_{\mathcal{M}^k}$ denotes the timestamp of the first error in module \mathcal{M}^k detected within the detection window (defined in Section 4.2.3). For the Perception module, we replace its results with bounding boxes retrieved from CARLA, ensuring that the module's outputs align with the ground truth. For the Prediction module, we obtain ground truth data from the collected dataset. Specifically, when rerunning a scenario s with its collected observations $\mathcal{O}(s)$, at time t , we retrieve the actual trajectory of the NPC object over the interval $[t, t + H_{\text{pred}}]$ from the simulator's observation $\mathcal{Y}(s) \in \mathcal{O}(s)$ and use this as the ground truth for the Prediction module. Considering the vast space of possible planned trajectories and control commands, we use the safest solution, which involves immediate braking, as the ground truth. This approach ensures that both the planning module and the control module consistently make the safest possible decisions.

5.2.2 Results. Table 4 presents the results for the correctness of *Module-Specific Oracle*. By replacing the module outputs with a safe ground truth, we observe that most of the detected MICs can be repaired, with average repair rates of 89.2%, 89.3%, 100% and 100% for the Perception, Prediction, Planning, and Control modules, respectively. These results demonstrate that our proposed *Module-Specific Oracle* can accurately identify the module-level root causes. Notably, the repair rates for the Perception and Prediction modules are not 100% (89.2% and 89.3%, respectively). This is primarily because these two modules are upstream; even when corrected with safe ground truth, it does not necessarily ensure that the downstream modules will continue to make safe decisions.

Answer to RQ2: *Module-Specific Oracle* can accurately identify the module whose errors are the root cause of safety-critical violations.

5.3 RQ3: Usefulness of *Module-Specific Feedback* and *Adaptive Seed Generation*

We assess the usefulness of key components in the fuzzing process in *MoDitector*, namely *Module-Specific Feedback* and *Adaptive Seed Generation*. To achieve this, we conducted a thorough evaluation by configuring a series of variants of *MoDitector* and then proceeded to evaluate their effectiveness. Currently, we verify this on the Prediction module.

Table 5. Results of ablation study on Prediction module.

Scenario	MoDitector	w/o Fine	w/o Coarse	w/o Select	w/o F-M	Random
S1	28.7	14.3	7.7	15.3	7.7	6.3
S2	24.3	17.0	13.3	20.7	15.7	11.3
S3	13.3	7.7	5.0	9.3	6.7	4.0
S4	9.0	2.7	1.3	7.7	3.0	1.7
Sum.	75.3	39.7	27.3	53	33	23.3

5.3.1 Module-Specific Feedback. To verify the effectiveness of feedback, we compare *MoDitector* with two variants: (1) *w/o F-M*, which removes the module-directed feedback from Eq. 9 to assess the impact of module-directed score on detecting MICSSs; (2) *Random*, which serves as a reference by reflecting the influence of the entire feedback mechanism on detecting MICSSs. As shown in Table 5, we find that *Random* generates the fewest MICSSs (23.3), underscoring the importance of the designed feedback. Comparing *w/o F-M* with *MoDitector*, we observe that *MoDitector* generates more MICSSs than *w/o F-M* (75.3 vs. 33), highlighting the value of module-directed feedback in detecting a greater number of MICSSs.

5.3.2 Adaptive Seed Generation. For *Adaptive Seed Generation*, we design three variants: (1) *w/o Fine*, which removes the fine-grained mutation from the adaptive mutation to evaluate the effectiveness of this mutation level; (2) *w/o Coarse*, similar to *w/o Fine*, but removes the coarse-grained mutation; and (3) *w/o Select*, which changes the adaptive seed selection to random seed selection to assess the usefulness of the adaptive mechanism. From the results shown in Table 5, we find that removing either the fine-grained mutation or the coarse-grained mutation reduces the number of detected MICSSs, with *w/o Fine* detecting only 41.7 MICSSs and *w/o Coarse* detecting 27.3 MICSSs. This demonstrates the effectiveness of our proposed adaptive mutation. By comparing *w/o Select* with *MoDitector*, we observe that *w/o Select* detects only 53 MICSSs, indicating that adaptive seed selection is an effective strategy for generating MICSSs.

Answer to RQ3: Both *Module-Specific Feedback* and *Adaptive Seed Generation* are useful for *MoDitector* in detecting MICSSs effectively.

5.4 RQ4: Performance of MoDitector

Table 6. Results of time performance in seconds (s). * denotes a negligible minimal value.

Method	Seed Selection	Mutation	Feedback	Simulation	Total
Random	0.01*	1.12	N/A	213.32	214.44
AVFuzzer	0.01*	1.99	0.01*	219.58	221.48
BehAVExplor	0.01*	1.64	1.09	212.03	214.76
MoDitector	0.01*	3.23	0.11	172.79	176.13

We further assess the time performance of different components in *MoDitector*, including the overhead of Seed Selection, Mutation, Feedback, and Simulation. Specifically, we analyze the average time required to process a scenario. Table 6 shows the overall results for all tools. From the results, we find that the simulation process occupies the majority of the time. For instance, on average, *MoDitector* takes 176.13 seconds to process a scenario, with 172.79 seconds (98.1%) spent running the scenario in the simulator. All tools spend negligible time on seed selection, as it is a simple sampling operation. For mutation, *MoDitector* requires more time than others due to the additional

overhead of dynamic mutation. Our feedback calculation takes an average of 0.11 seconds, which is faster than *BehAVExplor*. In summary, the computation time of *MoDitector* remains within an acceptable range.

Answer to RQ4: *MoDitector* demonstrates efficiency, with the majority of the time (98.1%) spent in the simulation phase, while the main algorithmic components consume approximately 3.34 seconds (1.9%) of the total processing time.

6 Discussion

This paper is the first to investigate ADS failures from module-level root causes. Although *MoDitector* can effectively and efficiently detect *MICSs*, there are several potential areas for improvement that warrant further discussion.

Non-*MICS* Failures In *MoDitector*, we employ a strict oracle to determine *MICS* by requiring that only one module fails before a collision occurs. Consequently, many failure scenarios are not classified as being caused by a specific module, rendering them non-*MICS* failures. However, in some non-*MICS* scenarios, if the ground truth for a specific module is provided, as demonstrated in RQ2, normal operation might resume. These potential *MICS* may warrant further investigation.

Future Works There are two potential directions for future work. (1) Currently, *MoDitector* only considers single-module analysis. However, our *MoDitector* can be easily extended to support the detection of *MICSs* induced by multiple modules, which we plan to explore in future work. (2) In our individual module metrics, we focus solely on safety as the metric. Nevertheless, evaluating the ADS from non-safety-critical aspects is also important. In future work, we will incorporate additional metrics to broaden the evaluation scope.

7 Threats to Validity

Internal Validity. The accuracy of Root Cause Analysis is critical for *MoDitector*, as it affects the evaluation of the generated test scenarios and serves as the foundation for the subsequent fuzzing process. To achieve the most precise detecting for *MICS*, we employ the strictest criterion: within the collision's effect window, there must be one and only one module that experiences an error for us to attribute the collision to that module's fault. Although this approach may not always result in a relatively high proportion of qualifying scenarios(see Section 5.1), it ensures that the collisions in the generated test scenarios are indeed associated with specific modules(see Section 5.2).

External Validity. Since different ADSs employ varying combinations of modules and each module implementation has its own strengths and weaknesses, the experimental results can only be fully guaranteed to be directly related to the specific ADS and its corresponding model under test. To address this limitation, we will subsequently conduct tests on different ADSs and replace the existing module implementations within the ADS to further explore and validate our approach.

8 Related Works

Root Cause Analysis for AI Systems Inspired by testing approaches in other AI systems[5, 24, 28, 39, 45–47], recent years have seen attempts to introduce root cause analysis into the testing of ADS and related robotic systems. Swarmbug[27] treats the AI system as a black box, and proposes *Degree of Causal Contribution* to measure how configurations affect the behaviour of the swarm robotics. In contrast, the *Module-Specific Oracle* in *MoDitector* focuses more on the outputs of individual modules within the system, allowing us to identify the root causes of issues at a finer granularity. RVPLAYER[11] and ROCAS[17] propose an algorithm that replays the accident scenarios and checks if the accident can be avoided by changing some parameters to locate the root cause. Compared to

the methods in these two works, our *Module-Specific Oracle* establishes analysis metrics for each module and develops a module-to-system mapper to address the challenge of module-level error measurement. This allows for the analysis to be conducted with just a single run of the accident scenario, making the process more efficient and accurate in identifying the MICS.

Search-based Scenario Generation for ADS Testing Search-based methods have become one of the most popular algorithms in scenario-based testing due to their ability to efficiently explore complex scenario spaces[12, 51]. From an algorithmic framework perspective, it can be categorized into evolutionary algorithm[7, 21, 25, 42, 52], model-based searching[16, 22, 23, 32, 50], and fuzzing methods[8–10, 18, 31, 36] which we use in *MoDetector*. Unlike these methods, *MoDetector* goes beyond efficiently generating collision or failure scenarios. It establishes a relationship between module errors and system failures, generating MICS for specific modules within the ADS. This approach is designed to better help ADS developers in enhancing their system components.

9 Conclusion

In this work, we introduce *MoDetector*, a fuzzing method to generate specific-module-sensitive test scenarios for ADS testing. *MoDetector* first build a root analysis function to locate which modules are corresponded to the collision. Building upon this function, *MoDetector* calculates root cause scores and customizes the seed selection and mutation modules accordingly. Extensive experiments are conducted with various primary scenarios, specific modules and fuzzing methods to validate the effectiveness of *MoDetector*. Experimental results demonstrate that *MoDetector* is highly effective in generating collision scenarios caused by errors in specific modules.

References

- [1] [n. d.]. GitHub - autowarefoundation/autoware: Autoware - the world's leading open-source software project for autonomous driving – github.com. <https://github.com/autowarefoundation/autoware>. [Accessed 08-Jul-2023].
- [2] Comma ai. 2023. Openpilot. <https://comma.ai/openpilot>
- [3] Karl Johan Åström, Tore Hägglund, Chang C Hang, and Weng K Ho. 1993. Automatic tuning and adaptation for PID controllers—a survey. *Control Engineering Practice* 1, 4 (1993), 699–714.
- [4] Baidu. 2023. Baidu-Apollo. <https://www.apollo.auto>
- [5] Shruti Bothe, Usama Masood, Hasan Farooq, and Ali Imran. 2020. Neuromorphic AI empowered root cause analysis of faults in emerging networks. In *2020 IEEE International Black Sea Conference on Communications and Networking (BlackSeaCom)*. IEEE, 1–6.
- [6] Mattias Brännström, Erik Coelingh, and Jonas Sjöberg. 2010. Model-based threat assessment for avoiding arbitrary vehicle collisions. *IEEE Transactions on Intelligent Transportation Systems* 11, 3 (2010), 658–669.
- [7] Alessandro Calò, Paolo Arcaini, Shaikat Ali, Florian Hauer, and Fuyuki Ishikawa. 2020. Generating avoidable collision scenarios for testing autonomous driving systems. In *2020 IEEE 13th International Conference on Software Testing, Validation and Verification (ICST)*. IEEE, 375–386.
- [8] Mingfei Cheng, Yuan Zhou, and Xiaofei Xie. 2023. Behavexplor: Behavior diversity guided testing for autonomous driving systems. In *Proceedings of the 32nd ACM SIGSOFT International Symposium on Software Testing and Analysis*. 488–500.
- [9] Mingfei Cheng, Yuan Zhou, and Xiaofei Xie. 2024. DriveTester: A Unified Platform for Simulation-Based Autonomous Driving Testing. *arXiv preprint arXiv:2412.12656* (2024).
- [10] Mingfei Cheng, Yuan Zhou, Xiaofei Xie, Junjie Wang, Guozhu Meng, and Kairui Yang. 2024. Evaluating Decision Optimality of Autonomous Driving via Metamorphic Testing. *arXiv preprint arXiv:2402.18393* (2024).
- [11] Hongjun Choi, Zhiyuan Cheng, and Xiangyu Zhang. 2022. RVPLAYER: Robotic Vehicle Forensics by Replay with What-if Reasoning. In *29th Annual Network and Distributed System Security Symposium, NDSS 2022*. The Internet Society.
- [12] Wenhao Ding, Chejian Xu, Mansur Arief, Haohong Lin, Bo Li, and Ding Zhao. 2023. A survey on safety-critical driving scenario generation—A methodological perspective. *IEEE Transactions on Intelligent Transportation Systems* (2023).
- [13] Alexey Dosovitskiy, German Ros, Felipe Codevilla, Antonio Lopez, and Vladlen Koltun. 2017. CARLA: An open urban driving simulator. In *Conference on robot learning*. PMLR, 1–16.
- [14] Electrek. 2023. Damning Footage Shows Tesla Vehicles on Autopilot Crashing into Police. <https://electrek.co/2023/08/09/damning-footage-shows-tesla-vehicles-autopi>

- [15] Jin Fang, Dingfu Zhou, Feilong Yan, Tongtong Zhao, Feihu Zhang, Yu Ma, Liang Wang, and Ruigang Yang. 2020. Augmented LiDAR simulator for autonomous driving. *IEEE Robotics and Automation Letters* 5, 2 (2020), 1931–1938.
- [16] Shuo Feng, Haowei Sun, Xintao Yan, Haojie Zhu, Zhengxia Zou, Shengyin Shen, and Henry X Liu. 2023. Dense reinforcement learning for safety validation of autonomous vehicles. *Nature* 615, 7953 (2023), 620–627.
- [17] Shiwei Feng, Yapeng Ye, Qingkai Shi, Zhiyuan Cheng, Xiangzhe Xu, Siyuan Cheng, Hongjun Choi, and Xiangyu Zhang. 2024. ROCAS: Root Cause Analysis of Autonomous Driving Accidents via Cyber-Physical Co-mutation. *arXiv preprint arXiv:2409.07774* (2024).
- [18] Weiwei Fu, Heqing Huang, Yifan Zhang, Ke Zhang, Jin Huang, Wei-Bin Lee, and Jianping Wang. 2024. ICSFuzz: Collision Detector Bug Discovery in Autonomous Driving Simulators. *arXiv preprint arXiv:2408.05694* (2024).
- [19] Ross Girshick, Jeff Donahue, Trevor Darrell, and Jitendra Malik. 2014. Rich feature hierarchies for accurate object detection and semantic segmentation. In *Proceedings of the IEEE conference on computer vision and pattern recognition*. 580–587.
- [20] Ionel Gog, Sukrit Kalra, Peter Schafhalter, Matthew A Wright, Joseph E Gonzalez, and Ion Stoica. 2021. Pylot: A modular platform for exploring latency-accuracy tradeoffs in autonomous vehicles. In *2021 IEEE International Conference on Robotics and Automation (ICRA)*. IEEE, 8806–8813.
- [21] Seunghee Han, Jaeuk Kim, Geon Kim, Jaemin Cho, Jiin Kim, and Shin Yoo. 2021. Preliminary evaluation of path-aware crossover operators for search-based test data generation for autonomous driving. In *2021 IEEE/ACM 14th International Workshop on Search-Based Software Testing (SBST)*. IEEE, 44–47.
- [22] Fitash Ul Haq, Donghwan Shin, and Lionel Briand. 2022. Efficient online testing for DNN-enabled systems using surrogate-assisted and many-objective optimization. In *Proceedings of the 44th international conference on software engineering*. 811–822.
- [23] Fitash Ul Haq, Donghwan Shin, and Lionel C Briand. 2023. Many-objective reinforcement learning for online testing of dnn-enabled systems. In *2023 IEEE/ACM 45th International Conference on Software Engineering (ICSE)*. IEEE, 1814–1826.
- [24] Md Abir Hossen, Sonam Kharade, Bradley Schmerl, Javier Cámara, Jason M O’Kane, Ellen C Czaplinski, Katherine A Dzurilla, David Garlan, and Pooyan Jamshidi. 2023. C a RE: Finding Root Causes of Configuration Issues in Highly-Configurable Robots. *IEEE Robotics and Automation Letters* 8, 7 (2023), 4115–4122.
- [25] Dmytro Humeniuk, Foutse Khomh, and Giuliano Antoniol. 2022. A search-based framework for automatic generation of testing environments for cyber-physical systems. *Information and Software Technology* 149 (2022), 106936.
- [26] Michael A Johnson and Mohammad H Moradi. 2005. *PID control*. Springer.
- [27] Chijung Jung, Ali Ahad, Jinho Jung, Sebastian Elbaum, and Yonghwi Kwon. 2021. Swarmbug: debugging configuration bugs in swarm robotics. In *Proceedings of the 29th ACM Joint Meeting on European Software Engineering Conference and Symposium on the Foundations of Software Engineering*. 868–880.
- [28] Taegyung Kim, Chung Hwan Kim, Altay Ozen, Fan Fei, Zhan Tu, Xiangyu Zhang, Xinyan Deng, Dave Jing Tian, and Dongyan Xu. 2020. From control model to program: Investigating robotic aerial vehicle accidents with {MAYDAY}. In *29th USENIX Security Symposium (USENIX Security 20)*. 913–930.
- [29] Friedrich Kruber, Jonas Wurst, and Michael Botsch. 2018. An unsupervised random forest clustering technique for automatic traffic scenario categorization. In *2018 21st International conference on intelligent transportation systems (ITSC)*. IEEE, 2811–2818.
- [30] lgsvl. 2022. LGSVL Sunsetting. <https://github.com/lgsvl/simulator>.
- [31] Guanpeng Li, Yiran Li, Saurabh Jha, Timothy Tsai, Michael Sullivan, Siva Kumar Sastry Hari, Zbigniew Kalbarczyk, and Ravishankar Iyer. 2020. Av-fuzzer: Finding safety violations in autonomous driving systems. In *2020 IEEE 31st international symposium on software reliability engineering (ISSRE)*. IEEE, 25–36.
- [32] Zhuo Li, Xiongfei Wu, Derui Zhu, Mingfei Cheng, Siyuan Chen, Fuyuan Zhang, Xiaofei Xie, Lei Ma, and Jianjun Zhao. 2023. Generative model-based testing on decision-making policies. In *2023 38th IEEE/ACM International Conference on Automated Software Engineering (ASE)*. IEEE, 243–254.
- [33] Guannan Lou, Yao Deng, Xi Zheng, Mengshi Zhang, and Tianyi Zhang. 2022. Testing of autonomous driving systems: where are we and where should we go?. In *Proceedings of the 30th ACM Joint European Software Engineering Conference and Symposium on the Foundations of Software Engineering*. 31–43.
- [34] Chen Ma, Ningfei Wang, Qi Alfred Chen, and Chao Shen. 2024. Slowtrack: Increasing the latency of camera-based perception in autonomous driving using adversarial examples. In *Proceedings of the AAAI Conference on Artificial Intelligence*, Vol. 38. 4062–4070.
- [35] Wassim G Najm, John D Smith, Mikio Yanagisawa, et al. 2007. *Pre-crash scenario typology for crash avoidance research*. Technical Report. United States. National Highway Traffic Safety Administration.
- [36] Qi Pang, Yuanyuan Yuan, and Shuai Wang. 2022. Mdpfuzz: testing models solving markov decision processes. In *Proceedings of the 31st ACM SIGSOFT International Symposium on Software Testing and Analysis*. 378–390.
- [37] Ashish Rana and Avleen Malhi. 2021. Building safer autonomous agents by leveraging risky driving behavior knowledge. In *2021 International Conference on Communications, Computing, Cybersecurity, and Informatics (CCCI)*. IEEE, 1–6.

- [38] Guodong Rong, Byung Hyun Shin, Hadi Tabatabaee, Qiang Lu, Steve Lemke, Mārtiņš Možeiko, Eric Boise, Geehoon Uhm, Mark Gerow, Shalin Mehta, et al. 2020. Lgsvl simulator: A high fidelity simulator for autonomous driving. In *2020 IEEE 23rd International conference on intelligent transportation systems (ITSC)*. IEEE, 1–6.
- [39] Jieke Shi, Zhou Yang, Junda He, Bowen Xu, Dongsun Kim, DongGyun Han, and David Lo. 2024. Finding Safety Violations of AI-Enabled Control Systems through the Lens of Synthesized Proxy Programs. *arXiv preprint arXiv:2410.04986* (2024).
- [40] Andrea Stocco, Paulo J Nunes, Marcelo d'Amorim, and Paolo Tonella. 2022. Thirdeye: Attention maps for safe autonomous driving systems. In *Proceedings of the 37th IEEE/ACM International Conference on Automated Software Engineering*. 1–12.
- [41] Andrea Stocco, Michael Weiss, Marco Calzana, and Paolo Tonella. 2020. Misbehaviour prediction for autonomous driving systems. In *Proceedings of the ACM/IEEE 42nd international conference on software engineering*. 359–371.
- [42] Yun Tang, Yuan Zhou, Tianwei Zhang, Fenghua Wu, Yang Liu, and Gang Wang. 2021. Systematic testing of autonomous driving systems using map topology-based scenario classification. In *2021 36th IEEE/ACM International Conference on Automated Software Engineering (ASE)*. IEEE, 1342–1346.
- [43] Eric Thorn, Shawn C Kimmel, Michelle Chaka, Booz Allen Hamilton, et al. 2018. *A framework for automated driving system testable cases and scenarios*. Technical Report. United States. Department of Transportation. National Highway Traffic Safety.
- [44] Robin van der Made, Martijn Tideman, Ulrich Lages, Roman Katz, and Martin Spencer. 2015. Automated generation of virtual driving scenarios from test drive data. In *24th International Technical Conference on the Enhanced Safety of Vehicles (ESV) National Highway Traffic Safety Administration*.
- [45] Zhijie Wang, Yuheng Huang, Lei Ma, Haruki Yokoyama, Susumu Tokumoto, and Kazuki Munakata. 2022. An Exploratory Study of AI System Risk Assessment from the Lens of Data Distribution and Uncertainty. *arXiv preprint arXiv:2212.06828* (2022).
- [46] Xuan Xie, Jiayang Song, Zhehua Zhou, Fuyuan Zhang, and Lei Ma. 2023. Mosaic: Model-based Safety Analysis Framework for AI-enabled Cyber-Physical Systems. *arXiv preprint arXiv:2305.03882* (2023).
- [47] Guangba Yu, Gou Tan, Haojia Huang, Zhenyu Zhang, Pengfei Chen, Roberto Natella, and Zibin Zheng. 2024. A Survey on Failure Analysis and Fault Injection in AI Systems. *arXiv preprint arXiv:2407.00125* (2024).
- [48] Qingzhao Zhang, Shengtuo Hu, Jiachen Sun, Qi Alfred Chen, and Z Morley Mao. 2022. On adversarial robustness of trajectory prediction for autonomous vehicles. In *Proceedings of the IEEE/CVF Conference on Computer Vision and Pattern Recognition*. 15159–15168.
- [49] Qingzhao Zhang, Shuwei Jin, Ruiyang Zhu, Jiachen Sun, Xumiao Zhang, Qi Alfred Chen, and Z Morley Mao. 2024. On data fabrication in collaborative vehicular perception: Attacks and countermeasures. In *33rd USENIX Security Symposium (USENIX Security 24)*. 6309–6326.
- [50] Ziyuan Zhong, Gail Kaiser, and Baishakhi Ray. 2022. Neural network guided evolutionary fuzzing for finding traffic violations of autonomous vehicles. *IEEE Transactions on Software Engineering* 49, 4 (2022), 1860–1875.
- [51] Ziyuan Zhong, Yun Tang, Yuan Zhou, Vania de Oliveira Neves, Yang Liu, and Baishakhi Ray. 2021. A survey on scenario-based testing for automated driving systems in high-fidelity simulation. *arXiv preprint arXiv:2112.00964* (2021).
- [52] Yuan Zhou, Yang Sun, Yun Tang, Yuqi Chen, Jun Sun, Christopher M Poskitt, Yang Liu, and Ziji Yang. 2023. Specification-based autonomous driving system testing. *IEEE Transactions on Software Engineering* 49, 6 (2023), 3391–3410.